Published in final edited form as:
Mol Microbiol. 2013 June ; 88(5): . doi:10.1111/mmi.12235.

RemA is a DNA-binding protein that activates biofilm matrix gene expression in *Bacillus subtilis*

Jared T. Winkelman[1], **Anna C. Bree**[2], **Ashley R. Bate**[3], **Patrick Eichenberger**[3], **Richard L. Gourse**[1], and **Daniel B. Kearns**[2,*]

[1]Department of Bacteriology, University of Wisconsin-Madison, Madison, WI 53706, USA.

[2]Department of Biology, Indiana University, Bloomington, IN 47405, USA.

[3]Center for Genomics and Systems Biology, Department of Biology, New York University, New York, NY 10003, USA.

Summary

Biofilm formation in *Bacillus subtilis* requires expression of the *eps* and *tapA-sipW-tasA* operons to synthesize the extracellular matrix components, extracellular polysaccharide and TasA amyloid proteins, respectively. Expression of both operons is inhibited by the DNA-binding protein master regulator of biofilm formation SinR and activated by the protein RemA. Here we show that RemA is a DNA-binding protein that binds to multiple sites upstream of the promoters of both operons and is both necessary and sufficient for transcriptional activation *in vivo* and *in vitro*. We further show that SinR negatively regulates *eps* operon expression by occluding RemA binding and thus for the P_{eps} promoter SinR functions as an anti-activator. Finally, transcriptional profiling indicated that RemA was primarily a regulator of the extracellular matrix genes, but it also activated genes involved in osmoprotection, leading to the identification of another direct target, the *opuA* operon.

Introduction

Many types of bacteria are capable of forming multicellular communities known as biofilms (O'Toole *et al.*, 2000; Branda *et al.*, 2005; Kolter and Greenberg, 2006). Cells within a biofilm cohere to one another and adhere to surfaces by producing an extracellular matrix often made of a species-specific composite of polysaccharides, proteins and nucleic acids (Flemming and Wingender, 2010). In addition, bacteria often inhibit flagellar motility concomitant with biofilm formation, perhaps to permit the formation of nucleation centres for aggregates or to stabilize aggregates once they have formed (Kolter and Greenberg, 2006). Biofilms are important factors in biofouling and pathogenesis. Understanding the complex regulation of extracellular matrix components and the inhibition of motility is important to combat biofilm formation in industrial and clinical settings.

One organism capable of forming biofilms is the Gram-positive model organism *Bacillus subtilis*. Under laboratory conditions, *B. subtilis* biofilms form structured pellicles at the liquid–air interface or colonies with complex architecture at the solid–air interface (Branda *et al.*, 2001). The biofilms consist of non-motile cells encased in an extracellular matrix

*For correspondence. dbkearns@indiana.edu; Tel. (+1) 812 856 2523; Fax (+1) 812 855 6705.

Supporting information
Additional supporting information may be found in the online version of this article at the publisher's web-site.

composed of an extracellular polysaccharide (EPS) tethered by the amyloid protein TasA and made hydrophobic by the amphiphilic protein BslA (Branda *et al.*, 2006; Guttenplan *et al.*, 2010; Romero *et al.*, 2010; Ostrowski *et al.*, 2011; Kobayashi and Iwano, 2012). The TasA protein is encoded within the *tapA-sipW-tasA* operon that also encodes the TapA protein and SipW signal peptidase, which are required for TasA anchoring and processing respectively (Branda *et al.*, 2004; Chu *et al.*, 2006; Romero *et al.*, 2011; Terra *et al.*, 2012). The EPS is synthesized by gene products resembling sugar-related enzymes encoded within the 15 gene *eps* operon (Branda *et al.*, 2001; Kearns *et al.*, 2005; Guttenplan *et al.*, 2010). Among the products encoded within the *eps* operon is the bifunctional glycosyltransferase EpsE that not only participates enzymatically in EPS synthesis but also inhibits motility by disengaging the flagellar rotor from the proton channels that power rotation (Blair *et al.*, 2008; Guttenplan *et al.*, 2010). Thus, regulation of the *eps* operon is sufficient to promote the motility-to-biofilm transition as *eps* expression results in biofilm matrix production and motility inhibition.

The *eps* and *tapA-sipW-tasA* operons are expressed by σ^A RNAP directed by the P_{eps} and P_{tapA} promoters respectively. Both the P_{eps} and P_{tapA} promoters are co-ordinately inhibited by SinR, a DNA-binding protein that serves as the master regulator for biofilm formation (Gaur *et al.*, 1991; Kearns *et al.*, 2005; Chu *et al.*, 2006; Colledge *et al.*, 2011). During biofilm initiation, SinR inhibition is relieved in a subpopulation of cells when the concentration of SinI exceeds a theoretical threshold, binds to SinR and prevents SinR binding to DNA (Bai *et al.*, 1993; Kearns *et al.*, 2005; Chai *et al.*, 2008). SinI antagonism of SinR also turns on *slrR*, a gene upstream and oppositely oriented from the *eps* operon, that encodes SlrR, a secondary SinR antagonist that further drives the cells into a biofilm forming state (Chu *et al.*, 2008; Chai *et al.*, 2010). Cells mutated for *sinR* are non-motile because of the constitutive expression of EPS synthesis and the motility inhibitor flagellar clutch protein EpsE (Blair *et al.*, 2008; Guttenplan *et al.*, 2010).A genetic screen to identify mutations that restored motility to a *sinR epsH* mutant identified loss of function mutations that disrupted EpsE and two other proteins, RemA and RemB, that regulated the extracellular matrix by activating the *eps*, *tapA* and *slrR* genes (Blair *et al.*, 2008; Winkelman *et al.*, 2009).

Here we elucidate the mechanism by which RemA regulates the production of the extracellular matrix. Despite the fact that RemA does not appear to encode a known DNA-binding motif, it nonetheless bound specifically to and activated transcription from the P_{eps} and P_{tapA} promoters *in vitro*. RemA bound to multiple sites upstream of both promoters and may cause bending of the DNA. Transcriptome analysis suggested that few genes besides those involved in the synthesis of the biofilm matrix were strongly regulated by RemA but we show that the *opuA* operon, required for glycine betaine uptake and osmoprotection, is also a direct RemA target. Finally, we show that SinR inhibits the *eps* operon by competing with RemA for binding and thereby mechanistically functions as an anti-activator. RemA and SinR appear to form two parallel but converging pathways suggesting that EPS and TasA activation in *B. subtilis* may be governed by at least two independent environmental inputs.

Results

RemA directly activates transcription of the eps operon

The P_{eps} promoter of the *eps* operon, necessary to synthesize the biofilm EPS, is inhibited by SinR and activated by RemA (Kearns *et al.*, 2005; Chu *et al.*, 2006; Winkelman *et al.*, 2009). Expression from a reporter in which the P_{eps} promoter was fused to the *lacZ* gene encoding β-galactosidase (P_{eps}–*lacZ*) increased 50-fold in the absence of the inhibitor SinR and was abolished in the absence of the SinR antagonist SinI or the activator protein RemA

(Fig. 1, grey bars) (Winkelman *et al.*, 2009). SinR, however, binds to the P_{eps} promoter from positions −78 to −52 relative to the transcriptional start site, which is too far upstream to occlude RNAP access, and the mechanism of RemA activation is unknown (Kearns *et al.*, 2005). To explore P_{eps} regulation further, an 'improved' promoter was generated in which the third position in the P_{eps} −35 hexamer was mutated towards consensus for σ^A RNAP (TTTTAA to TTGTAA) and fused to *lacZ*. Expression from the improved reporter ($P_{eps}^{improved}$–*lacZ*) was increased in all genetic backgrounds tested and expression was restored to near wild-type levels even in the absence of SinI and RemA (Fig. 1, black bars). We conclude that improving the P_{eps} promoter closer to consensus relieves both the inhibition by SinR and the requirement for RemA.

Mutation of RemA was epistatic to mutation of SinR with respect to expression from the P_{eps}–*lacZ* reporter (Fig. 1, Winkelman *et al.*, 2009). One way to explain the epistasis is if RemA was a transcriptional activator and SinR served as an anti-activator. To determine whether RemA activates transcription directly, we conducted *in vitro* transcription reactions with σ^A-containing RNAP holoenzyme, in the presence and absence of a purified RemA-maltose-binding protein fusion (RemA–MBP). Transcription from a plasmid template containing the P_{eps} or $P_{eps}^{improved}$ promoter was strongly enhanced in the presence of RemA–MBP (Fig. 2A). Activation was specific for RemA–MBP, as a control protein fusion of β-galactosidase to maltose-binding protein (LacZ–MBP) failed to increase expression from the P_{eps} promoter (Fig. 2A).Addition of SinR abolished RemA-dependent activation but did not abolish basal expression from the $P_{eps}^{improved}$ promoter (Fig. 2A). We conclude that RemA acts as a transcriptional activator of P_{eps} both *in vivo* and *in vitro*. We further conclude that SinR does not formally inhibit the P_{eps} core promoter but rather acts as a RemA anti-activator.

To determine whether RemA-dependent transcriptional activation was promoter-specific, we tested whether RemA–MBP could activate expression from a plasmid containing the heterologous *Escherichia coli* promoter, *lacUV5*. Expression from *lacUV5* was unaffected by RemA–MBP, indicating that activation by RemA was specific to sequences found in the P_{eps} promoter (Fig. 2A). The promoter sequence determinants for activation were identified by creating nested 5' deletions upstream of P_{eps} in the context of the plasmid template used for the *in vitro* transcription reactions. There was no difference in the level of activation by RemA–MBP when there were 452 bp, 176 bp or 159 bp of P_{eps} sequence upstream of the *eps* transcriptional start site. There was a decrease in the ability of RemA–MBP to activate transcription, however, when only 121 bp of upstream sequence was present and a complete loss of RemA-dependent activation when only 107 bp of upstream sequence was present (Fig. 2B). We conclude that RemA requires, at least in part, a specific DNA sequence between 107 and 159 bp upstream of the P_{eps} transcription start site for full activation by RemA.

Most transcription factors specifically regulate expression of their target genes by binding to specific DNA sequences in or near the target promoters (Browning and Busby, 2004). To directly test if RemA specifically bound to DNA we carried out electrophoretic mobility shift assays (EMSAs) with purified RemA–MBP and radiolabelled DNA containing P_{eps} promoter fragments. The migration of the P_{eps} promoter fragment was shifted by RemA–MBP concentrations of 0.5 μM or greater (Fig. 3A). In contrast, RemA–MBP did not shift a control fragment containing the *rrnB* P1 promoter at any concentration tested (≤ 0.9 μM; Fig. 3B). We conclude that RemA is a DNA-binding protein that binds to sequences upstream of specific promoters. The change from no binding to binding occurred in a very narrow range of RemA concentrations, suggesting that RemA binding might be cooperative (Fig. 3A).

To determine where RemA bound relative to the P_{eps} core promoter, DNase I footprint analysis was performed. Increasing concentrations of RemA–MBP were added to radiolabelled P_{eps}-containing DNA, and the resulting complexes were subjected to nucleolytic cleavage by DNase I. Addition of RemA–MBP at 0.5 μM resulted in protection from approximately −110 to −50 on P_{eps}, but the pattern of protection was periodic: 7 bp regions of protection were separated by 3 bp of unaltered, or even enhanced, digestion (Figs 4A and 5). Based on these data, RemA appeared to bind to at least six sites (BS1–BS6) upstream of the P_{eps} core promoter within the region required for RemA-dependent stimulation of *in vitro* transcription (Figs 2B and 5). We also note that at high concentrations, RemA-dependent protection extended to positions closer to the transcriptional start site than −49 (Fig. 4A). Although we could not map these lower affinity sites to high resolution, they may be near the predicted position of RNAP binding. Finally, the presence of 0.4 μM SinR abolished all RemA-dependent protections and enhancements, and instead led to protection that corresponded to the known SinR binding sites that overlapped with RemA BS1 and BS2 (Figs 4A and 5; Kearns *et al.*, 2005). We conclude that RemA binds in a specific pattern upstream of the *Peps* promoter and that SinR served as an anti-activator by occluding RemA binding.

To determine the contributions of the RemA binding sites to gene activation, we first took an unbiased forward genetic approach. The P_{eps} promoter was randomly mutagenized by low fidelity PCR, cloned in front of a promoterless *lacZ* gene encoding β-galactosidase and inserted in the ectopic chromosomal *amyE* locus of a strain mutated for SinR and EpsH. SinR was mutated to relieve inhibition of the P_{eps} promoter and EpsH was mutated to circumvent the severe cell aggregation associated with P_{eps} expression that can result in loss of colony-forming units. In this genetic background, colonies with wild-type P_{eps} promoter expression were blue on media containing the chromogenic β-galactosidase substrate X-gal due to high level expression of the reporter. Out of 1600 colonies screened, 16 white colonies were clonally isolated and the P_{eps} promoters fused to the *lacZ* reporter were sequenced. After discarding non-unique mutations, six independent mutant alleles were isolated. Four of the alleles that disrupted expression (*eps14, eps15, eps40, eps41*) were mutations found within the −35 and −10 promoter elements of P_{eps} (Fig. 5). The fifth allele (*eps32*) was a deletion of a single T residue immediately upstream of the −35 sequence and the sixth allele (*eps33*) was a mutation in a region protected by RemA (BS6) (Fig. 5). Overall, few mutations were identified within the putative RemA binding sites perhaps because cooperative binding at some sites buffers against subtle changes at others.

Next, we took a reverse genetic approach to determine the contributions of the RemA binding sites upstream of the P_{eps} promoter. Two deletion mutations were generated by allelic replacement: $P_{eps}\Delta^{remsite34}$ deleted the regions of RemA protection BS3 and BS4, and $P_{eps}\Delta^{remsite56}$ deleted regions of RemA protection BS5 and BS6 (Fig. 5). Both Δ*remsite34* and Δ*remsite56* deletions abolished expression from corresponding P_{eps} promoter fragments in *in vitro* transcription assays (Fig. 2C). Finally, the Δ*remsite34* and Δ*remsite56* mutations had severe biofilm defects that phenocopied a *remA* mutation in an otherwise wild-type background (Fig. 6). We conclude that the BS3, BS4, BS5 and BS6 regions of P_{eps} bound by RemA are critical for transcriptional activation of the *eps* operon *in vitro* and biofilm formation *in vivo*.

RemA activates and binds to promoters expressing the tasA and opuA operons

RemA is also required for the activation of the P_{tapA} promoter that drives expression of the *tapA-sipW-tasA* operon responsible for synthesis of the amyloid protein component of the *B. subtilis* biofilm matrix (Branda *et al.*, 2006; Chu *et al.*, 2006). As with the P_{eps} promoter, RemA– MBP activated *in vitro* transcription from a vector containing the P_{tapA} promoter region and caused an electrophoretic mobility shift of a P_{tapA}-containing DNA fragment

within a narrow range of protein concentration (Figs 2A and 3C). DNase I footprinting assays showed that RemA– MBP protected multiple regions upstream of the P_{tapA} promoter with a periodicity reminiscent of that observed with the P_{eps} promoter (Fig. 4B). Unlike P_{eps} however, RemA binding was not occluded upstream of the SinR binding site and both SinR and RemA bound simultaneously (Fig. 4B). SinR was previously shown to bind both upstream and downstream of the P_{tapA} promoter and probably represses P_{tapA} expression by occluding promoter access (Chu *et al.*, 2006). We conclude that RemA directly and co-ordinately activates both operons that encode structural components of the *B. subtilis* biofilm matrix but that SinR acts as an anti-activator for P_{eps} and a repressor for P_{tapA}.

To identify additional genes under RemA control we conducted transcriptional profiling comparing RNA from cells mutated for *remA*, *sinR* and *epsH* and cells mutated for *sinR* and *epsH* alone. The *sinR* mutation was introduced to relieve repression of potential RemA-activated genes that could mask the full effect of RemA on expression, and the *epsH* mutation was introduced to prevent cell clumping in the *sinR* background that can obscure cell density measurements. Consistent with previous reports, genes in the *eps* and *tapA* operons were activated 100-fold by RemA and these operons experienced the strongest level of transcriptional control in the regulon (Table 1). In addition, a number of other genes were activated including three operons involved in the uptake of the osmoprotectants glycine betaine and choline, *opuA*, *opuB* and *opuC*, which were expressed substantially higher in the presence of RemA (Kempf and Bremer, 1995; Kappes *et al.*, 1999). Relatively few genes were repressed by RemA (Table 2). We infer from the strongest genes regulated by RemA that the primary function of RemA is to regulate extracellular matrix (*rem*) gene expression consistent with its name.

The next strongest RemA regulatory effect after the biofilm matrix genes, was the 40-fold activation of the *opuA* operon. Regulation of *opuA* by RemA also appeared to be direct as purified RemA–MBP caused an electrophoretic mobility shift of the P_{opuA} promoter region in a concentration range similar to that observed with the P_{eps} and P_{tapA} promoters (Fig. 3D). Likewise, RemA–MBP protected DNA in a periodic repeating pattern reminiscent of the P_{eps} and P_{tapA} promoters (Fig. 4C). Unlike P_{eps} and P_{tapA}, however, RemA–MBP was not sufficient to activate expression from a P_{opuA} containing fragment in the *in vitro* transcription assay (Fig. 2A). Also different from P_{eps} and P_{tapA}, increasing concentrations of SinR had no effect on the pattern of RemA-dependent DNase I digestion on P_{opuA} and there were no SinR-dependent protections or enhancements of cutting (Fig. 4C). We conclude that RemA directly activates P_{opuA} expression *in vivo* but is not sufficient for activation *in vitro* perhaps suggesting that other regulatory factors may be required. We further conclude that not all genes activated by RemA are regulated by SinR.

Together, RemA bound to three different promoters and protected at least 17 regions of DNA that could be determined from the DNase I protection assays (Fig. 4; Fig. S1A). We attempted to determine a RemA consensus binding sequence from the regions of protection. Because the RemA binding sites did not appear to be clear discrete dyads, it was difficult to determine whether the binding sites represented a series of tandem inverted repeats or a series of direct repeats. The best alignment was obtained if the repeats were considered to be direct and a consensus prediction was conducted using Weblogo (Crooks *et al.*, 2004). If the regions are in fact direct repeats, we predict that the consensus RemA binding site is AGNAAAA (Fig. S1B). We note that the consensus sequence is rather weak and often poorly conserved in each individual binding site, again perhaps owing to the apparently high level of cooperativity of RemA binding to DNA.

Discussion

The regulation of biofilm formation in *B. subtilis* is complex. SinR is a DNA-binding protein that co-ordinately binds to and represses expression of genes that encode the biofilm matrix (Kearns *et al.*, 2005; Chu *et al.*, 2006). Spo0A, a response regulator, both indirectly antagonizes SinR and inhibits the biofilm repressor AbrB, whereas DegU, another response regulator, activates expression of the matrix component BslA (Hamon *et al.*, 2004; Kobayashi, 2007; Verhamme *et al.*, 2007; Chai *et al.*, 2011; Ostrowski *et al.*, 2011). In addition, RemA and RemB are required to activate expression of matrix genes but their mechanism was unknown as they lacked helix–turn–helix motifs (Winkelman *et al.*, 2009). Here we demonstrate that RemA is a DNA-binding protein that is both necessary and sufficient for the activation of the P_{eps} and P_{tapA} promoters that express the matrix biosynthesis *eps* and *tapA-sipW-tasA* operons respectively. Furthermore, transcriptional profiling indicated the matrix operons were the strongest RemA targets but also lead to the discovery that RemA regulates expression of operons involved in osmoprotection. Finally, we show that the master regulator SinR represses the *eps* operon by antagonizing the binding of RemA and therefore mechanistically functions as an anti-activator.

RemA bound to DNA with apparently high cooperativity and protected at least six regions upstream of both the P_{eps} and P_{tapA} promoters from DNase I digestion. We interpret each of the protected regions as a series of individual, direct repeat binding sites with a weak consensus of AGNAAAA that are perhaps compensated for by cooperative binding. Each direct repeat was separated by 3 bp of either unprotected or enhanced DNase I digestion. Enhancements of digestion are usually due to bending distortions that widen the major groove of DNA and increase the affinity of DNase I (Weston *et al.*, 1992). We infer from the periodicity of DNase I protection and enhancement that RemA is binding to one face of the double helix and bending the DNA. DNA bending has been shown to be essential for some transcription factors to function (Gosink *et al.*, 1993). How DNA bending promotes RemA-dependent activation is unclear but we note that the promoter-proximal binding site is precisely 16 bp upstream of the −35 elements for both P_{eps} and P_{tapA} (Fig. S1). Furthermore, deletion of a single base upstream of the P_{eps} −35 element was sufficient to abolish expression (*eps32*, Fig. 5). While the strict spacing between the two elements in the two promoters may be coincidental, it may suggest that the face of DNA to which RemA binds relative to the promoter is important for activation.

In addition to the matrix biosynthesis operons, we discovered that RemA also directly activates the *opuA* operon that encodes genes for the uptake of the osmoprotectant glycine betaine (Boch *et al.*, 1994; Kempf and Bremer, 1995). High osmotic pressure may be experienced by cells in a biofilm due to the production of the extracellular matrix and perhaps osmoprotection operons are co-induced by RemA to physiologically compensate for matrix synthesis (Rubinstein *et al.*, 2012). Whereas mutants defective in the RemA-matrix targets EpsH and TasA have severe biofilm defects, cells defective in OpuA formed biofilms like the wild type (Fig. 6). Biofilm defects in OpuA may only be detectable in environments with glycine betaine or the absence of OpuA may be compensated for by two other RemA-activated osmolyte uptake systems OpuB and OpuC (Kappes *et al.*, 1999). Expression of the *opuA* operon is activated by high external salt concentrations and is inhibited by the osmoprotectants proline and glycine betaine but the regulators that mediate these transcriptional effects are unknown (Kempf and Bremer, 1995; Steil *et al.*, 2003; Hoffmann *et al.*, 2013). Whether RemA is responsible for the osmotic regulation of *opuA* is unknown but we note that DNA topology modulation by bending and twist, like that seemingly caused by RemA, has been implicated in the regulation of osmoprotection genes in other organisms (Hulton *et al.*, 1990; Wang and Syvanen, 1992).

Systems-level transcriptomics suggests that expression of *remA* is nearly uniform save a decrease during late sporulation (Nicolas *et al.*, 2012). Thus, we infer that the physiological input that controls RemA-dependent gene expression may occur at the level of RemA activity. Based on the regulation of the osmoprotection operons and the connection to the biofilm matrix, high osmolarity is one potential stimulus. Alternatively, RemA could respond to nitrogen levels or availability as a substantial number of genes related to nitrogen metabolism were modestly induced in the RemA transcriptional profiling experiment (Table 1). Phylogenetically, the RemA protein is both highly conserved and broadly distributed being encoded within the genomes of Firmicutes, Thermotogales, Cyanobacteria, δ-proteobacteria and Chloroflexi (Fig. S2A). The relationship of these diverse bacteria to one another is unclear but we explored the genetic neighbourhood surrounding RemA for further insight. In each genome we examined, RemA was encoded immediately upstream of the *gmk* gene encoding the Gmk guanylate kinase perhaps suggesting a connection between RemA and the cytoplasmic pool of GTP (Fig. S2B). Many bacteria form biofilms but the environmental and physiological signals that instruct biofilm formation is seldom known. In the case of *B. subtilis*, activation of the biofilm matrix genes appears to require the integration of at least two signals, one to antagonize SinR and the other to activate RemA.

Experimental procedures

Growth conditions

Bacillus subtilis strains were grown in Luria–Bertani (LB) (10 g tryptone, 5 g yeast extract, 5 g NaCl per litre) broth or on LB plates fortified with 1.5% Bacto agar at 37°C. When appropriate, antibiotics were included at the following concentrations: 10 μg ml^{-1} tetracycline, 100 μg ml^{-1} spectinomycin, 5 μg ml^{-1} chloramphenicol, 5 μg ml^{-1} kanamycin and 1 μg ml^{-1} erythromycin plus 25 μg ml^{-1} lincomycin (*mls*). Isopropyl (β-D-thiogalactopyranoside (IPTG, Sigma) was added to the medium at the indicated concentration when appropriate.

For pellicle formation experiments, 10 μl of culture grown overnight at room temperature in LB medium was inoculated into 10 ml minimal MSgg medium [5 mM potassium phosphate (pH 7), 100 mM MOPS (pH 7), 2 mM $MgCl_2$, 700 μM $CaCl_2$, 50 μM $MnCl_2$, 50 μM $FeCl_3$, 1 μM $ZnCl_2$, 2 μM thiamine, 0.5% glycerol, 0.5% glutamate, 50 μg ml^{-1} tryptophan, 50 μg ml^{-1} phenylalanine and 50 μg ml^{-1} threonine] in six-well microtitre plates and incubated at 25°C (Branda *et al.*, 2001). For colony architecture analysis, colonies were toothpick inoculated onto minimal MSgg medium fortified with 1.5% Bacto agar and incubated for 3 days at 25°C.

Strain construction

All constructs were first introduced into the domesticated strain PY79 by natural competence and then transferred to the 3610 background using SPP1-mediated generalized phage transduction (Yasbin and Young, 1974). All strains used in this study are listed in Table 3. All plasmids used in this study are listed in Supplemental Table S1. All primers used in this study are listed in Supplemental Table S2.

opuA::tet—The *opuA::tet* insertion deletion allele was generated using a modified 'Gibson' isothermal assembly protocol (Gibson *et al.*, 2009). Briefly, the region upstream of *opuAA* was PCR-amplified using the primer pair 3318/3319 and the region downstream of *opuAC* was PCR-amplified using the primer pair 3320/3321. DNA containing a tetracycline resistance gene (pDG1515; Guérout-Fleury *et al.*, 1995) was amplified using universal primers 3250/3251. The three DNA fragments were combined at equimolar amounts to a total volume of 5 μl and added to a 15 μl aliquot of prepared master mix (see below). The

reaction was incubated for 60 min at 50°C. The completed reaction was then PCR-amplified using primers 3318/3321 to amplify the assembled product. The amplified product was transformed into competent cells of PY79 and then transferred to the 3610 background using SPP1-mediated generalized transduction. Insertions were verified by PCR amplification using primers 3318/3321.

A 5× isothermal assembly reaction buffer [500 mM Tris-HCL pH 7.5, 50 mM $MgCl_2$, 50 mM DTT (Bio-Rad), 31.25 mM PEG-8000 (Fisher Scientific), 5.02 mM NAD (Sigma Aldrich) and 1 mM of each dNTP (New England BioLabs)] was aliquoted and stored at −80°C. An assembly master mixture was made by combining prepared 5× isothermal assembly reaction buffer (131 mM Tris-HCl, 13.1 mM $MgCl_2$, 13.1 mM DTT, 8.21 mM PEG-8000, 1.32 mM NAD and 0.26 mM each dNTP) with Phusion DNA polymerase (New England BioLabs) (0.033 units μl^{-1}), T5 exonuclease diluted 1:5 with 5× reaction buffer (New England BioLabs) (0.01 units μl^{-1}), *Taq* DNA ligase (New England BioLabs) (5328 units μl^{-1}) and additional dNTPs (267 μM). The master mix was aliquoted as 15 μl and stored at −80°C.

Markerless deletions—To generate the Δ*remsite34* marker-less deletion construct, the region upstream of *remsite34 was* PCR-amplified using the primer pair 2713/2714 and digested with EcoRI and XhoI, and the region downstream of *remsite1* was PCR-amplified using the primer pair 2716/2718 and digested with XhoI and BamHI. The two fragments were then simultaneously ligated into the EcoRI and BamHI sites of pMiniMAD2 which carries a temperature-sensitive origin of replication and an erythromycin resistance cassette to generate pDP376 (Patrick and Kearns, 2008). The plasmid pDP376 was introduced to 3610 by rare single-cross-over integration by transformation at the restrictive temperature for plasmid replication (37°C) using *mls* resistance as a selection. To evict the plasmid, the strain was incubated in 3 ml LB broth at a permissive temperature for plasmid replication (22°C)for 14 h. Cells were then serially diluted and plated on LB agar at 37°C. Individual colonies were patched on LB plates and LB plates containing *mls* to identify *mls*-sensitive colonies that had evicted the plasmid. Chromosomal DNA from colonies that had excised the plasmid was purified, PCR-amplified with primers 2713/2718, and screened by digestion with XhoI to determine which isolate had retained the *remsite34* allele.

To generate the Δ*remsite56* marker-less deletion construct, the region upstream of *remsite1* was PCR-amplified using the primer pair 2713/2715 and digested with EcoRI and XhoI, and the region downstream of *remsite56* was PCR-amplified using the primer pair 2717/2718 and digested with XhoI and BamHI. The two fragments were then simultaneously ligated into the EcoRI and BamHI sites of pMiniMAD2 which carries a temperature-sensitive origin of replication and an erythromycin resistance cassette to generate pDP377. The plasmid pDP377 was integrated, excised, and the Δ*remsite56* allele was verified as described above for Δ*remsite34*.

LacZ reporter construct—To generate the *amyE::*$P_{eps}^{improved}$*– lacZ* β-galactosidase reporter construct pRLG12296, −452 to +35 of $P_{eps}^{improved}$ was amplified from plasmid pRLG11810 using primers 4831/6097, digested with EcoRI and BamHI and cloned into the EcoRI and BamHI site of pDG268 which carries a chloramphenicol-resistance marker and a polylinker upstream of the *lacZ* gene between two arms of the *amyE* gene (Guérout-Fleury *et al.*, 1996).

MBP–RemA expression construct—The *remA* gene was PCR-amplified using primer pair 1527/1528 and 3610 chromosomal DNA, digested with EcoRI and BamHI and cloned into the EcoRI/BamHI sites of plasmid pMAL-c2X (New England Biolabs) to generate plasmid pKB116.

***In vitro* transcription plasmids—**All promoters studied using *in vitro* transcription were PCR-amplified from NCIB3610 chromosomal DNA, digested with EcoRI and HindIII, and ligated into the EcoRI and HindIII sites of pRLG770 (Ross *et al.*, 1990). To generate pRLG11810, −452 to +35 of P_{epsA} was amplified using primers 4831 and 5619. To generate pRLG12760, −176 to +35 of P_{epsA} was amplified with primers 6157 and 5619. To generate pRLG12759, −159 to +35 of P_{epsA} was amplified using primers 6158 and 5619. To generate pRLG12764, −121 to +35 of P_{epsA} was amplified using primers 6159 and 5619. To generate, p12757, −107 to +35 of P_{epsA} was amplified using primers 5620 and 5619. To generate pRLG12786, −168 to +65 of P_{tapA} was amplified using primers 6463 and 6464. To generate pRLG12784, −172 to +27 of P_{opuA} P1 (−135 to +64 of P_{opuA} P2) was amplified from 3610 chromosomal DNA using primers 6465 and 6466. To generate the $P_{epsA}^{improved}$, pRLG11810 was mutagenized using primer 5892 to generate plasmid pRLG11825.

Plasmids for fragment labelling—To generate pRLG7340 *E. coli rrnB* P1 promoter DNA was amplified from pRLG1616 using primers 4633 and 1620, digested with EcoRI and HindIII and ligated into EcoRI and HindIII digested pSL6. To generate RLG12766, −159 to +35 of P_{eps} was amplified from NCIB3610 chromosomal DNA using primers 6158 and 5619, digested with EcoRI and HindIII and ligated into digested pSL6. To generate pRLG12783, −172 to +27 of P_{opuA} was amplified from NCIB3610 chromosomal DNA using primers 6465 and 6466, digested with EcoRI and HindIII and ligated into digested pSL6. To generate pRLG12785, −168 to +65 of P_{tapA} was amplified from NCIB3610 chromosomal DNA using primers 6463 and 6464, digested with EcoRI and HindIII, and ligated into digested pSL6.

SPP1 phage transduction

To 0.2 ml of dense culture grown in TY broth (LB broth supplemented after autoclaving with 10 μM $MgSO_4$ and 100 μM $MnSO_4$), serial dilutions of SPP1 phage stock were added and statically incubated for 15 min at 37°C. To each mixture, 3 ml TYSA (molten TY supplemented with 0.5% agar) was added, poured atop fresh TY plates, and incubated at 37°C overnight. Top agar from the plate containing near confluent plaques was harvested by scraping into a 50 ml conical tube, vortexed and centrifuged at 5000 *g* for 10 min. The supernatant was treated with 25 μg ml^{-1} DNase final concentration before being passed through a 0.45 μm syringe filter and stored at 4°C.

Recipient cells were grown to stationary phase in 2 ml TY broth at 37°C. 0.9 ml cells were mixed with 5 μl of SPP1 donor phage stock. Nine millilitres of TY broth was added to the mixture and allowed to stand at 37°C for 30 min. The transduction mixture was then centrifuged at 5000 *g* for 10 min, the supernatant was discarded and the pellet was resuspended in the remaining volume. One hundred microlitres of cell suspension was then plated on TY fortified with 1.5% agar, the appropriate antibiotic and 10 mM sodium citrate.

Protein purification

SinR was purified as previously described (Kearns *et al.*, 2005) His-tagged SinR was overexpressed from plasmid pDP91 in BL21(DE3) cells. One litre of culture was grown in LB supplemented with 30 μg ml^{-1} kanamycin at 37°C until OD_{600} of 0.5 was obtained. IPTG was added to 1 mM and the cells were shifted to 22°C and grown for 3 h before harvesting by centrifugation. The cell pellet was resuspended in 40 ml lysis buffer (50 mM Tris-Cl pH 8.5, 500 mM NaCl, 10 mM imidazole 0.1 mM PMSF) and the cells were lysed by sonication. Cell debris was cleared by centrifugation and the resulting supernatant was applied to a column with 1 ml of NiNTA slurry that had been equilibrated in lysis buffer. The column was washed with 10 ml of wash buffer (50 mM Tris-Cl pH 8.5, 500 mM NaCl, 20 mM imidazole) and eluted with 1 ml of elution buffer (10 mM Tris-Cl pH 8.5, 10 mM

$MgCl_2$, 1 mM EDTA, 300 mM DTT, 5% glycerol). To cleave the His-tag from SinR 3 μl of 0.9 U μl^{-1} biotinylated thrombin (Novagen) was added and gently mixed overnight at room temperature before applying to a column with 0.5 ml of NiNTA agarose bead slurry equilibrated in elution buffer. One hundred micro-litres of streptavidin agarose was added to the eluate and gently mixed for 1 h before applying to a column. The eluate was dialysed against 10 mM Tris-Cl pH 8.5, 10 mM $MgCl_2$, 1 mM EDTA, 0.3 mM DTT, 50% glycerol, 1 mM PMSF.

RemA–MBP and LacZ–MBP were overproduced from plasmids pKB116 and pMal-c2X, respectively, in BL21(DE3) cells. Cells were grown in 1 l of LB supplemented with 0.2% glucose and 100 μg ml^{-1} ampicillin at 37°C to an OD_{600} of 0.5 before adding IPTG to 0.3 mM. The cells were grown for 2 more hours at 37°C before harvesting by centrifugation. Cell pellets were resuspended in 25 ml column buffer (20 mM Tris-Cl pH 7.4, 200 mM NaCl, 10 mM β-mercaptoethanol, 1 mM EDTA) and lysed by sonication. After clearing cell debris by centrifugation, the supernatant was loaded onto 1 ml slurry of amylose resin (NEB) that had been equilibrated in column buffer. The beads were washed with 12 ml of column buffer before eluting in 0.4 ml steps of elution buffer (column buffer + 10 mM maltose). Appropriate fractions were dialysed into RemA–MBP storage buffer (50 mM Tris-Cl pH 8.0, 150 mM NaCl, 0.1 mM EDTA, 1 mM DTT).

Bacillus subtilis RNAP, histidine-tagged on the β' subunit (Qi and Hulett, 1998), was purified from strain MH5636 similar to how it was previously described (Anthony *et al.*, 2000). MH5636 cells were grown in 4 l of LB to an OD_{600} of 1.0 before harvesting by centrifugation. The pellet was resuspended in 55 ml buffer P (300 mM NaCl, 50 mM Na_2HPO_4, 3 mM 2-mercaptoethanol, 5% glycerol, 1 mM PMSF) and cells were lysed by sonication followed by centrifugation. The supernatant was mixed with 5 ml of NiNTA slurry (Qiagen) that had been equilibrated in buffer P and gently mixed for 30 min at 4°C before applying to a polyprep column. The beads were washed with 60 ml of buffer P followed by washing with 60 ml buffer P +30 mM imidazole. Core RNAP was eluted in 1 ml steps with Buffer P +400 mM imidazole. Appropriate fractions were dialysed into storage buffer [50 mM Tris-Cl (8.0), 0.1 M NaCl, 3 mM 2-mercaptoethanol, 50% glycerol]. The σ^A subunit was a generous gift of Libor Krasny and had been purified as described (Juang and Helmann, 1994; López de Saro *et al.*, 1999). Core RNAP and σ^A were reconstituted in storage buffer (50 mM Tris-HCl pH 8.0, 0.1 M NaCl, 3 mM 2-mercaptoethanol, 50% glycerol) for 30 min at 30°C using 20-fold molar excess of σ^A. Titration experiments were carried out to ensure saturation of core RNAP.

In vitro transcription

Twenty-five microlitres of reactions containing 50 ng supercoiled plasmid DNA (plasmid templates used for *in vitro* transcription are listed in Supplemental Table S1) were pre-incubated 1 min at 22°C with the appropriate combinations of 700 nM RemA–MBP, 700 nM LacZ–MBP and/or 400 nM SinR in 10 mM Tris-Cl pH 8.0, 100 mM KCl, 10 mM $MgCl_2$, 1 mM DTT, 0.1 mg ml^{-1} BSA (NEB) 500 μM ATP, 200 μM GTP, 200 μM CTP, 0.1 μM UTP and [α-^{32}P]-UTP (PerkinElmer). Transcription was initiated by addition of purified RNA polymerase holoenzyme to a final concentration of 20 nM. Reactions were terminated after 15 min of incubation at 22°C by the addition of 25 μl of 95% formamide, 0.05% bromophenol blue and 0.025% xylene cyanole. Fifteen-microlitre aliquots of these reactions were electrophoresed on 5.5% acrylamide, 7 M urea, 1× TBE gels for 1.5 h at 200 V. The relative yield of transcript was determined using ImageQuant.

DNase I footprinting

The DNase I footprinting protocol was adapted from Bartlett *et al.* (1998). Plasmids pRLG12766 (containing a P_{epsA} promoter fragment, end-points −159 to +35), pRLG12785 (containing *PtapA* promoter fragment, end-points −168 to +65) or pRLG12783 (containing P_{opuAA} promoter fragment end-points −170 to +27) were digested with NcoI (NEB), end-labelled by filling-in with [α-^{32}P]-dCTP (Perkin-Elmer) using Sequenase (USB), and digested with NheI (NEB). The DNA was purified after each step by ethanol precipitation. The promoter fragments were run on a 5% acrylamide, 0.5× TBE gel for 1.5 h before being excised and diffused into low-salt Elutip-D buffer (0.2 M NaCl, 20 mM, Tris-Cl pH 7.4, 1 mM EDTA) O/N at 4°C. The DNA was purified using Elutip-D columns (Whatman), ethanol precipitated, and resuspended in 100 µl 10 mM Tris-HCl, pH 8.0. 125–1000 nM RemA–MBP (or RemA–MBP storage buffer) was added to ~ 0.2 nM template DNA in transcription buffer (10 mM Tris-HCl, pH 8.0, 30 mM KCl, 10 mM $MgCl_2$, 1 mM DTT, 0.1 µg µl^{-1} BSA) for 10 min at 22°C. One microlitre of DNase I (to a final concentration of 1 µg ml^{-1}) was added for 30 s before the reaction was stopped by addition of 10 mM EDTA and 0.3 M sodium acetate. The samples were phenol extracted and the DNA was precipitated with ethanol, washed with 100% ethanol, dried and suspended in 5 µl loading buffer (7 M urea, 0.5× TBE 0.05% bromophenol blue, 0.025% xylene cyanole). Reactions were electrophoresed on 8.5% acrylamide, 7 M urea, 0.5× TBE gels for 2.5 h at 2000 V.

Electrophoretic motility shift assays

Radiolabelled DNA fragments were purified as above. 100–900 nM RemA–MBP (or RemA–MBP storage buffer) was added to ~0.2nM template DNA in transcription buffer (10 mM Tris-HCl, pH 8.0, 30 mM KCl, 10 mM $MgCl_2$, 1 mM DTT, 0.1 µg µl^{-1} BSA) for 10 min at 22°C. DNA load dye was added and the reactions were electrophoresed on 5% acrylamide, 0.5× TBE gels for 1 h at 200 V.

Transcriptional profiling

Custom Agilent DNA microarrays were designed using the Agilent eArray application. The arrays include 15 744 60-mer probes which consist of the annotated protein-coding genes of the *B. subtilis* str. 168 genome, as well as the known non-coding RNAs entered into NCBI and reported in Rasmussen *et al.*, 2009 and Irnov *et al.*, 2010. Each protein-coding gene includes three probes and the non-coding RNAs have either two or three probes.

Bacillus subtilis strains DS207 and DS9771 were grown in LB at 37°C to an optical density of 1.0–1.1 at OD_{600} and samples were immediately mixed with an equal volume of methanol (−20°C) and centrifuged to pellet cells. Cell pellets were stored at −80°C. RNA was isolated using a hot acid-phenol isolation procedure as described above. The sample is then treated with Qiagen's RNase-Free DNase in solution and the RNA clean-up protocol of Qiagen's RNeasy® kit was used. The quality of the RNA was checked by visualizing the integrity of the 23S and 16S rRNA bands on an agarose gel.

Labelled cDNA was generated from RNA using Agilent's Fairplay® III Microarry Labelling Kit. The Agilent Two-Colour Microarray-Based Prokaryotic Analysis (FairPlay III Labelling) Protocol was used with the following changes: between 6 and 10 µg total RNA was used, the reverse transcription reaction was performed at 42°C for 2 h, and the NHS-ester dye-coupling reaction to amino allyl dUTP (using GE Healthcare Cy™3 and Cy™5 monofunctional reactive dyes) was incubated for 90 min. Hybridizations were incubated at 65°C for 17 h. Arrays were scanned by Agilent Technologies DNA Microarray Scanner with Surescan High-Resolution Technology.

Data were subjected to standard lowess normalization using Bioconductor and run in R was performed on the processed signal given by the Agilent software and the geometric mean of the probes was used to give the final value for each gene and nc-RNA.

Supplementary Material

Refer to Web version on PubMed Central for supplementary material.

Acknowledgments

We would like to thank Kris Blair for technical support and Patricia Sanchez-Vazquez for critical reading of the manuscript. This work was supported by NIH Training Grants NIH T32 GM07215 for J.W. and GM007757 for A.B., and by NIH Grants GM37048 to R.L.G., GM092616 to P.E. and GM093030 to D.B.K.

References

Anthony LC, Artsimovitch I, Svetlov V, Landick R, Burgess RR. Rapid purification of His(6)-tagged *Bacillus subtilis* core RNA polymerase. Protein Expr Purif. 2000; 19:350–354. [PubMed: 10910724]

Bai U, Mandic-Mulec I, Smith I. SinI modulates the activity of SinR, a developmental switch protein of *Bacillus subtilis*, by protein–protein interaction. Genes Dev. 1993; 7:139–148. [PubMed: 8422983]

Bartlett MS, Gaal T, Ross W, Gourse RL. RNA polymerase mutants that destabilize RNA polymerase-promoter complexes alter NTP-sensing by *rrn* P1 promoters. J Mol Biol. 1998; 279:331–345. [PubMed: 9642041]

Blair KM, Turner L, Winkelman JT, Berg HC, Kearns DB. A molecular clutch disables flagella in the *Bacillus subtilis* biofilm. Science. 2008; 320:1636–1638. [PubMed: 18566286]

Boch J, Kempf B, Bremer E. Osmoregulation in *Bacillus subtilis*: synthesis of the osmoprotectant glycine betaine from exogenously provided choline. J Bacteriol. 1994; 176:5364–5371. [PubMed: 8071213]

Branda SS, González-Pastor JE, Ben-Yehuda S, Losick R, Kolter R. Fruiting body formation by *Bacillus subtilis* . Proc Natl Acad Sci USA. 2001; 98:11621–11626. [PubMed: 11572999]

Branda SS, González-Pastor JE, Dervyn E, Ehrlich SD, Losick R, Kolter R. Genes involved in formation of structured multicellular communities by *Bacillus subtilis* . J Bacteriol. 2004; 186:3970–3979. [PubMed: 15175311]

Branda SS, Vik A, Friedman L, Kolter R. Biofilms: the matrix revisited. Trends Microbiol. 2005; 13:20–26. [PubMed: 15639628]

Branda SS, Chu F, Kearns DB, Losick R, Kolter R. A major protein component of the *Bacillus subtilis* biofilm matrix. Mol Microbiol. 2006; 59:1229–1238. [PubMed: 16430696]

Browning DF, Busby SJW. The regulation of bacterial transcription initiation. Nat Rev Microbiol. 2004; 2:57–65. [PubMed: 15035009]

Chai Y, Chu F, Kolter R, Losick R. Bistability and biofilm formation in *Bacillus subtilis* . Mol Microbiol. 2008; 67:254–263. [PubMed: 18047568]

Chai Y, Norman T, Kolter R, Losick R. An epigenetic switch governing daughter cell separation in *Bacillus subtilis* . Genes Dev. 2010; 24:754–765. [PubMed: 20351052]

Chai Y, Norman T, Kolter R, Losick R. Evidence that metabolism and chromosome copy number control mutually exclusive cell fates in *Bacillus subtilis* . EMBO J. 2011; 30:1402–1413. [PubMed: 21326214]

Chu F, Kearns DB, Branda SS, Kolter R, Losick R. Targets of the master regulator of biofilm formation in *Bacillus subtilis* . Mol Microbiol. 2006; 59:1216–1228. [PubMed: 16430695]

Chu F, Kearns DB, McLoon A, Chai Y, Kolter R, Losick R. A novel regulatory protein governing biofilm formation in *Bacillus subtilis* . Mol Microbiol. 2008; 68:1117–1127. [PubMed: 18430133]

Colledge VL, Fogg MJ, Levdikov VM, Leech A, Dodson EJ, Wilkinson AJ. Structure and organization of SinR, the master regulator of biofilm formation in *Bacillus subtilis* . J Mol Biol. 2011; 411:597–613. [PubMed: 21708175]

Crooks GE, Hon G, Chandonia JM, Brenner SE. Weblogo: a sequence logo generator. Genome Res. 2004; 14:1188–1190. [PubMed: 15173120]

Flemming H-C, Wingender J. The biofilm matrix. Nat Rev Microbiol. 2010; 8:623–633. [PubMed: 20676145]

Gaur NK, Oppenheim J, Smith I. The *Bacillus subtilis sin* gene, a regulator of alternative developmental processes, codes for a DNA-binding protein. J Bacteriol. 1991; 173:678–686. [PubMed: 1898931]

Gibson DG, Young L, Chuang R-Y, Venter JC, Hutchinson CA III, Smith HO. Enzymatic assembly of DNA molecules up to several hundred kilobases. Nat Methods. 2009; 6:343–345. [PubMed: 19363495]

Gosink KK, Ross W, Leirmo S, Osuna R, Finkel SE, Johnson RC, Gourse RL. DNA binding and bending are necessary but not sufficient for Fis-dependent activation of *rrnB* P1. J Bacteriol. 1993; 175:1580–1589. [PubMed: 8449867]

Guérout-Fleury AM, Shazand K, Frandsen N, Stragier P. Antibiotic-resistance cassettes for *Bacillus subtilis* . Gene. 1995; 167:335–336. [PubMed: 8566804]

Guérout-Fleury AM, Frandsen N, Stragier P. Plasmids for ectopic integration in *Bacillus subtilis* . Gene. 1996; 180:57–61. [PubMed: 8973347]

Guttenplan SB, Blair KM, Kearns DB. The EpsE flagellar clutch is bifunctional and synergizes with EPS biosynthesis to promote *Bacillus subtilis* biofilm formation. PLoS Genet. 2010; 6:e1001243. [PubMed: 21170308]

Hamon MA, Stanley NR, Britton RA, Grossman AD, Lazazzera BA. Identification of AbrB-regulated genes involved in biofilm formation by *Bacillus subtilis* . Mol Microbiol. 2004; 52:847–860. [PubMed: 15101989]

Hoffmann T, Wensing A, Brosius M, Steil L, Völker U, Bremer E. Osmotic control of *opuA* expression in *Bacillus subtilis* and its modulation in response to intracellular glycine betaine and proline pools. J Bacteriol. 2013; 195:510–522. [PubMed: 23175650]

Hulton CSJ, Seirafi A, Hinton JCD, Sidebotham JM, Waddell L, Pavitt GD, et al. Histone-like protein H1 (H-NS), DNA supercoiling and gene expression in bacteria. Cell. 1990; 63:631–642. [PubMed: 2171779]

Irnov I, Sharma CM, Vogel J, Winkler WC. Identification of regulatory RNAs in *Bacillus subtilis* . Nucleic Acids Res. 2010; 38:6637–6651. [PubMed: 20525796]

Juang YL, Helmann JD. The delta subunit of *Bacillus subtilis* RNA polymerase. An allosteric effector of the initiation and core-recycling phases of transcription. J Mol Biol. 1994; 239:1–14. [PubMed: 7515111]

Kappes RM, Kempf B, Kneip S, Boch J, Gade J, Meier-Wagner J, Bremer E. Two evolutionarily closely related ABC transporters mediate the uptake of choline for synthesis of the osmoprotectant glycine betaine in *Bacillus subtilis* . Mol Microbiol. 1999; 32:203–216. [PubMed: 10216873]

Kearns DB, Losick R. Cell population heterogeneity during growth of *Bacillus subtilis* . Genes Dev. 2005; 19:3083–3094. [PubMed: 16357223]

Kearns DB, Chu F, Branda SS, Kolter R, Losick R. A master regulator for biofilm formation by *Bacillus subtilis* . Mol Microbiol. 2005; 55:739–749. [PubMed: 15661000]

Kempf B, Bremer E. OpuA, an osmotically regulated binding protein-dependent transport system for the osmoprotectant glycine betaine in *Bacillus subtilis* . J Biol Chem. 1995; 270:16701–16713. [PubMed: 7622480]

Kobayashi K. Gradual activation of the response regulator DegU controls serial expression of genes for flagellum formation and biofilm formation in *Bacillus subtilis* . Mol Microbiol. 2007; 66:395–409. [PubMed: 17850253]

Kobayashi K, Iwano M. BslA(YuaB) forms a hydrophobic layer on the surface of *Bacillus subtilis* biofilms. Mol Microbiol. 2012; 85:51–66. [PubMed: 22571672]

Kolter R, Greenberg EP. The superficial life of microbes. Nature. 2006; 441:300–302. [PubMed: 16710410]

López de Saro FJ, Yoshikawa N, Helmann JD. Expression, abundance, and RNA polymerase binding properties of the delta factor of *Bacillus subtilis* . J Biol Chem. 1999; 274:15953–15958. [PubMed: 10336502]

Nicolas P, Mäder U, Dervyn E, Rochat T, Leduc A, Pigeonneau N, et al. Condition-dependent transcriptome reveals high-level regulatory architecture in *Bacillus subtilis* . Science. 2012; 335:1103–1106. [PubMed: 22383849]

O'Toole G, Kaplan HB, Kolter R. Biofilm formation as microbial development. Annu Rev Microbiol. 2000; 54:49–79. [PubMed: 11018124]

Ostrowski A, Mehert A, Prescott A, Kiley TB, Stanley-Wall NR. YuaB functions synergistically with the exopolysaccharide and TasA amyloid fibers to allow biofilm formation by *Bacillus subtilis* . J Bacteriol. 2011; 193:4821–4831. [PubMed: 21742882]

Patrick JE, Kearns DB. MinJ (YvjD) is a topological determinant of cell division in *Bacillus subtilis* . Mol Microbiol. 2008; 70:1166–1179. [PubMed: 18976281]

Qi Y, Hulett FM. PhoP-P and RNA polymerase sigmaA holoenzyme are sufficient for transcription of Pho regulon promoters in *Bacillus subtilis*: Pho-P activator sites within the coding region stimulate transcription *in vitro* . Mol Microbiol. 1998; 28:1187–1197. [PubMed: 9680208]

Rasmussen S, Nielsen HB, Jarmer H. The transcriptionally active regions in the genome of *Bacillus subtilis* . Mol Microbiol. 2009; 73:1043–1057. [PubMed: 19682248]

Romero D, Aguilar C, Losick R, Kolter R. Amyloid fibers provide structural integrity to *Bacillus subtilis* biofilms. Proc Natl Acad Sci USA. 2010; 107:2230–2234. [PubMed: 20080671]

Romero D, Vlamakis H, Losick R, Kolter R. An accessory protein required for anchoring and assembly of amyloid fibers in *B. subtilis* biofilms. Mol Microbiol. 2011; 80:1155–1168. [PubMed: 21477127]

Ross W, Thompson JF, Newlands JT, Gourse RL. *E. coli* Fis protein activates ribosomal RNA transcription *in vitro* and *in vivo* . EMBO J. 1990; 9:3733–3742. [PubMed: 2209559]

Rubinstein SM, Kolodkin-Gal I, McLoon A, Kolter R, Losick R, Weitz DA. Osmotic pressure can regulate matrix gene expression in *Bacillus subtilis* . Mol Microbiol. 2012; 86:426–436. [PubMed: 22882172]

Serizawa M, Yamamoto H, Yamaguchi H, Fujita Y, Kobayashi K, Ogasawara N, Sekiguchi J. Systematic analysis of SigD-regulated genes in *Bacillus subtilis* by DNA microarray and Northern blotting analyses. Gene. 2004; 329:125–136. [PubMed: 15033535]

Steil L, Hoffmann T, Budde I, Völker U, Bremer E. Genome-wide transcriptional profiling analysis of adaptation of *Bacillus subtilis* to high salinity. J Bacteriol. 2003; 185:6358–6370. [PubMed: 14563871]

Terra R, Stanley-Wall NR, Cao G, Lazazzera BA. Identification of *Bacillus subtilis* SipW as a bifunctional signal peptidase that controls surface-adhered biofilm formation. J Bacteriol. 2012; 194:2781–2790. [PubMed: 22328672]

Verhamme DT, Kiley TB, Stanley-Wall NR. DegU co-ordinates multicellular behavior exhibited by *Bacillus subtilis* . Mol Microbiol. 2007; 65:554–568. [PubMed: 17590234]

Wang J-Y, Syvanen M. DNA twist as a transcriptional sensor for environmental changes. Mol Microbiol. 1992; 6:1861–1866. [PubMed: 1508037]

Weston SA, Lahm A, Suck D. X-ray structure of the DNase I-d(GGTATACC)2 complex at 2.3 Å resolution. J Mol Biol. 1992; 226:1237–1256. [PubMed: 1518054]

Winkelman JT, Blair KM, Kearns DB. RemA(YlzA) and RemB(YaaB) regulate extracellular matrix operon expression and biofilm formation in *Bacillus subtilis* . J Bacteriol. 2009; 191:3981–3991. [PubMed: 19363116]

Yasbin RE, Young FE. Transduction in *Bacillus subtilis* by bacteriophage SPP1. J Virol. 1974; 14:1343–1348. [PubMed: 4214946]

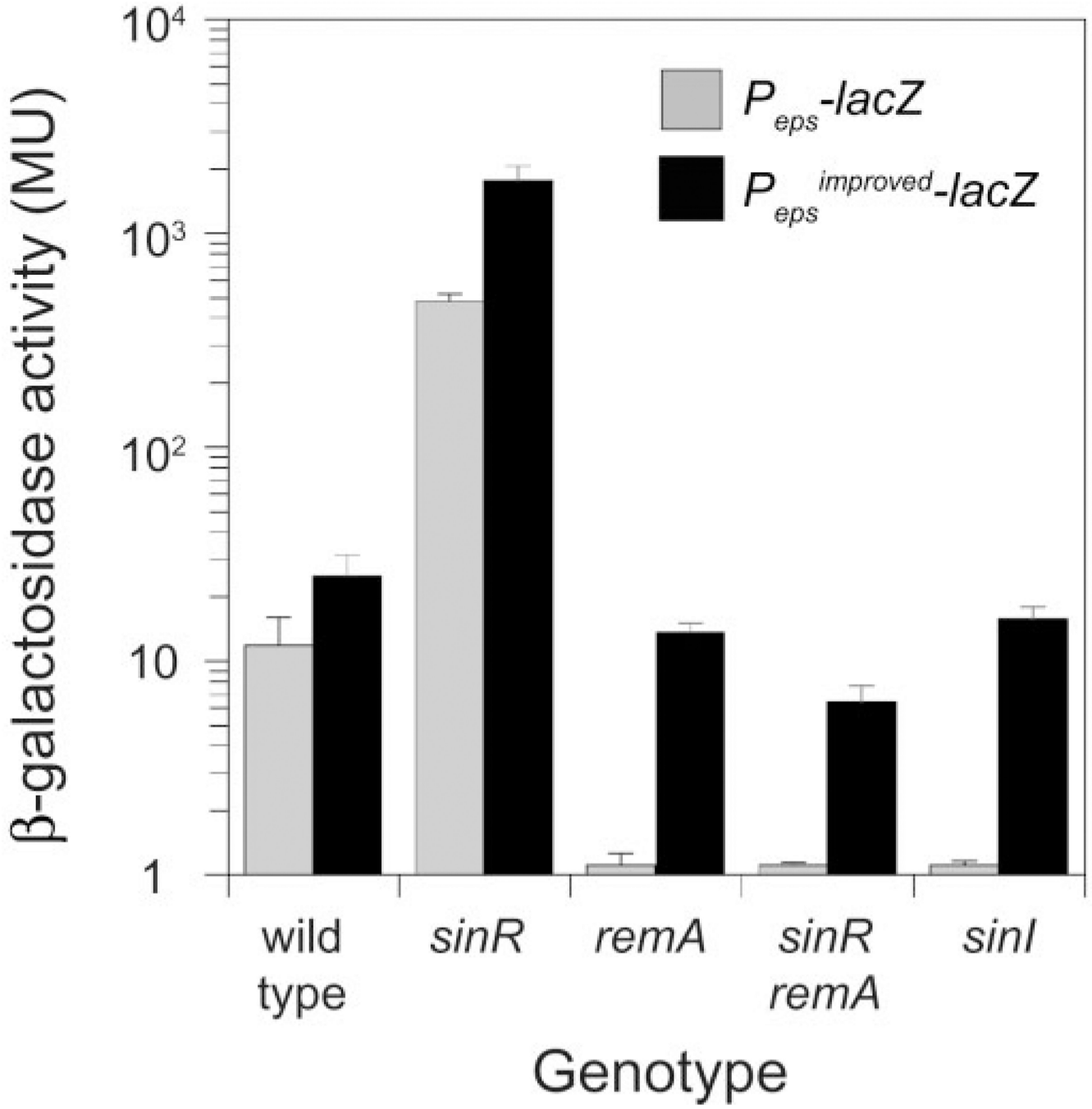

Fig. 1.

RemA activates P_{eps} expression *in vivo*. β-Galactosidase activity of P_{eps}–*lacZ* (grey bars) and $P_{eps}^{improved}$–*lacZ* (black bars) are presented for the indicated genotypes. Error bars are the standard deviations of data from three replicates. Raw data are presented in Table S3 in Supporting information. The following strains were used to generate this figure: wild type (DS1882, DS9468), *sinR* (DS2609, DS9467), *remA* (DS2913, DS9469), *sinR remA* (DS2911, DS9466) and *sinI* (DS444, DK445).

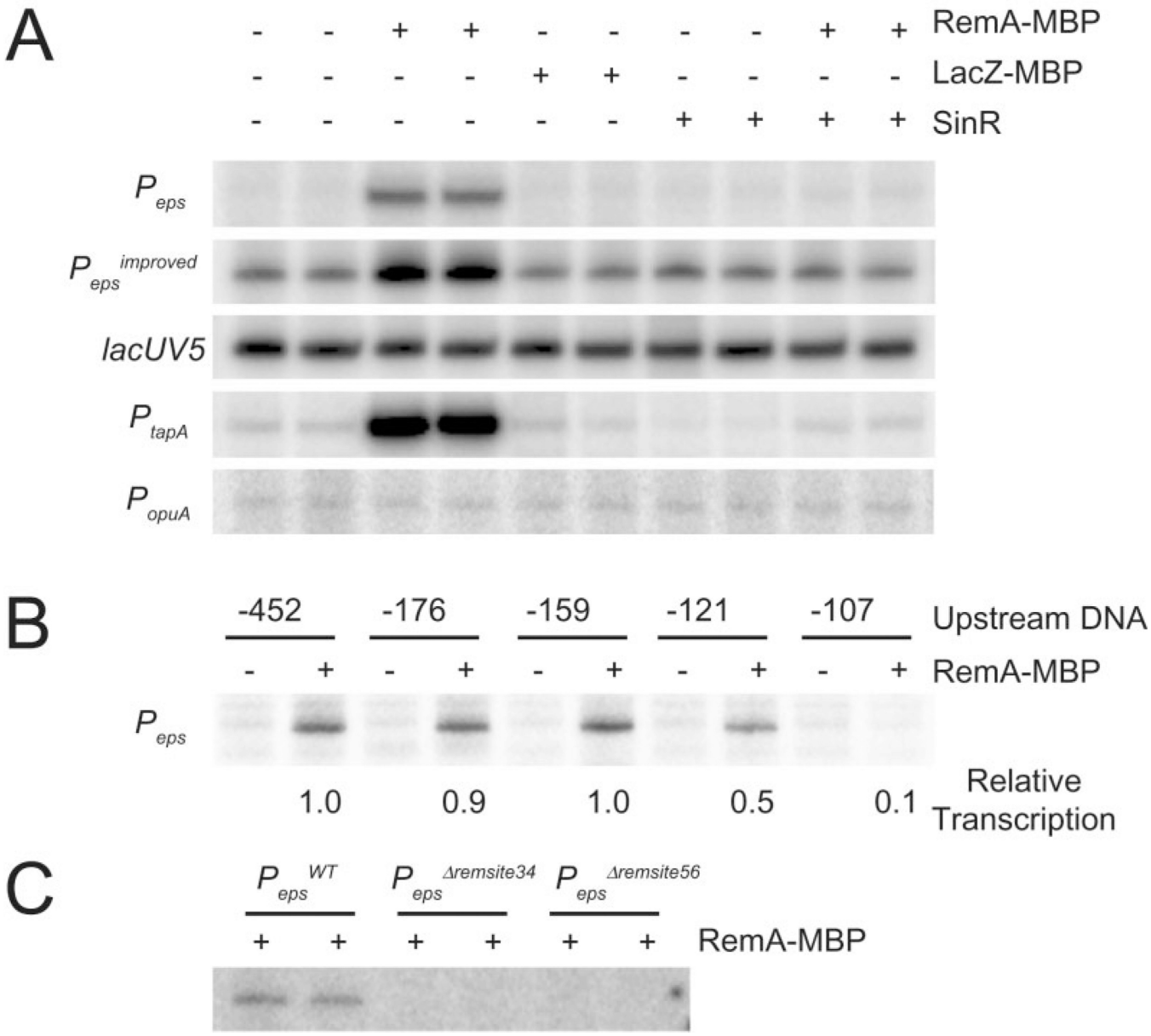

Fig. 2.

RemA activates transcription from specific promoters *in vitro. In vitro* transcription reactions were carried out in 100 mM KCl with 20 nM σ^A containing RNAP holoenzyme and 50 ng of supercoiled plasmid DNA with the indicated promoters cloned upstream of tandem transcription terminators.

A. RemA–MBP (700 nM), LacZ–MBP (700 nM) or SinR (400 nM) were added to *in vitro* transcription reactions containing the followingpromoters cloned upstream of tandem transcription terminators: P_{eps} (−452 to +35), $P_{eps}^{improved}$ (−452 to +35 with the −35 element changed from TTTAAA to TTGAAA), *lacUV5* (−60 to +40), P_{tapA} (−168 to +65) or P_{opuA} (−173 to +26).

B. *In vitro* transcription reactions were carried out with supercoiled plasmid containing P_{eps} promoter DNA with the indicated number of nucleotides upstream of the transcription start site cloned upstream of tandem transcription terminators. The downstream promoter end-point was +35 in each case. RemA–MBP (700 nM) or RemA–MBP storage buffer were

added to each reaction. Relative transcription was determined by dividing the intensity in each lane by the intensity in lane 2. The indicated values for relative transcription are the averages from three different experiments.

C. *In vitro* transcription reactions were carried out with supercoiled plasmid containing 700 nM RemA–MBP and either WT P_{eps} (−452 to +35)or P_{eps} promoter fragments containing the indicated Δ*remsite34* or Δ*remsite56* deletions.

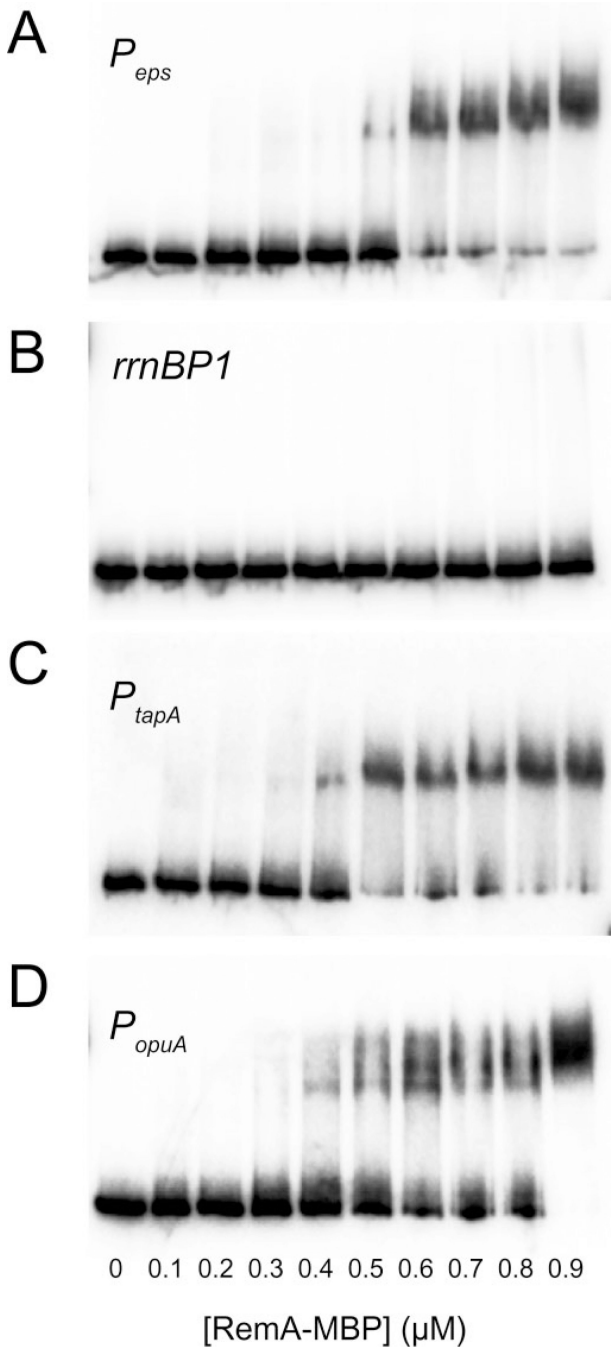

Fig. 3.

RemA binds to specific promoters. 5'-Radiolabelled DNA containing the indicated promoters were incubated with the indicated concentrations of RemA–MBP and electrophoresed under non-denaturing conditions. The size of each DNA fragment and the promoter end-points, respectively, were: (A) 252 bp containing P_{eps} from −159 to +35; (B) 182 bp containing *rrnB* P1 from −73 to +50; (C) 291 bp containing P_{tapA} from−168 to +65; and (D) 258 bp containing P_{opuA} DNA from −172 to +27 (P_{opuA} P2 from −135 to +64).

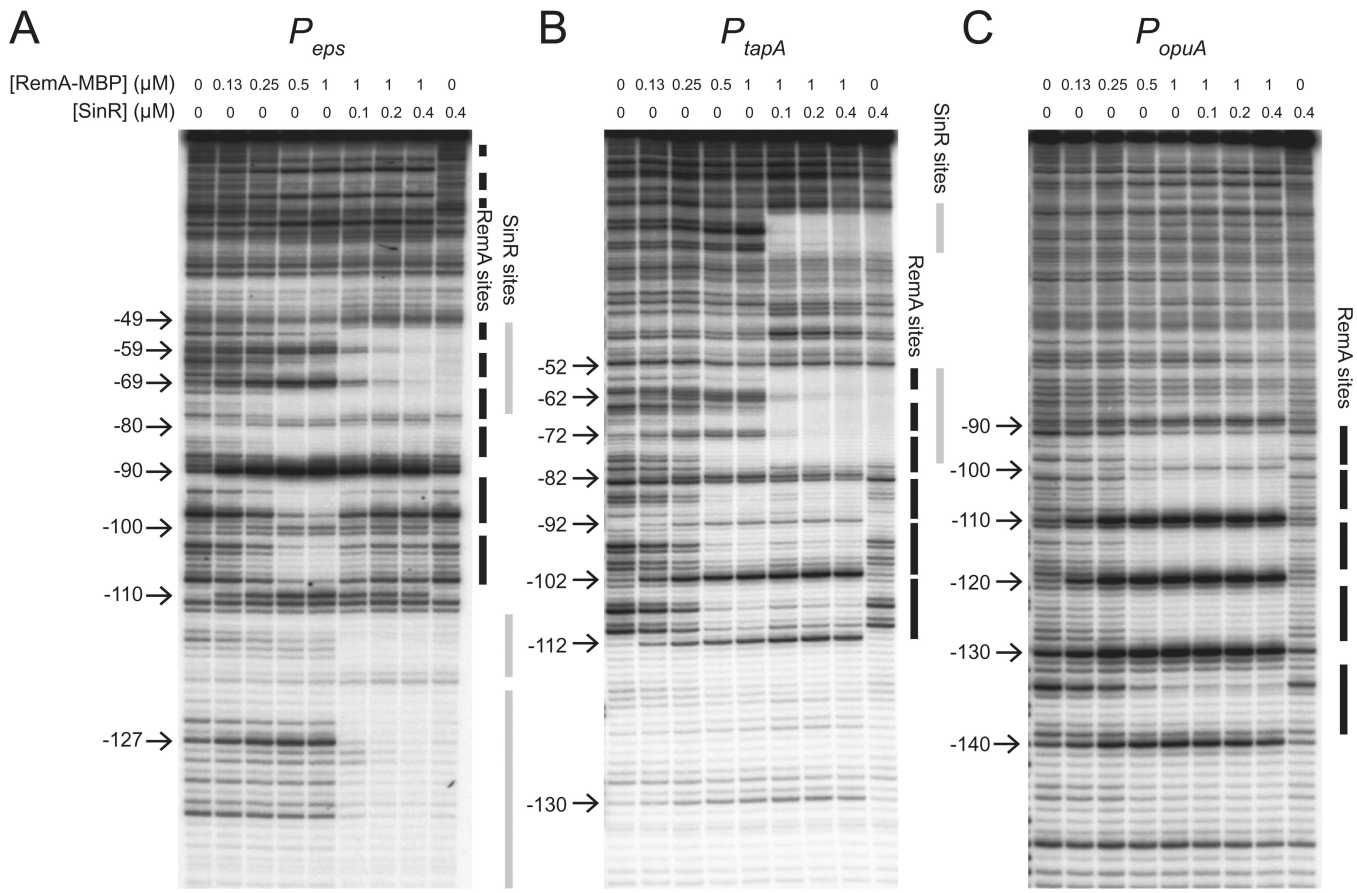

Fig. 4.

RemA binds to multiple sites in target promoters. 5'-Radiolabelled DNA containing the indicated promoters was incubated with RemA–MBP, RemA–MBP storage buffer and/or SinR at the indicated concentrations before treating the samples with DNase I. Positions of cutting relative to the transcription start site are indicated on the left of each gel and were determined using an A+G sequence ladder specific for each DNA fragment (not shown). Regions protected from DNase I digestion by RemA–MBP are indicated as vertical black bars. Regions protected from DNase I digestion by SinR are indicated as vertical grey bars.

Fig. 5.

Summary of RemA binding sites and other relevant P_{eps} landmarks. The sequence of the P_{eps} promoter and intergenic region between the *slrR* gene and the *eps* operon is arranged from 5' at the upper left to 3' at the lower right. The *slrR* and *epsA* genes are indicated as grey arrows. SinR binding sites (SinR BS), the −35 box and −10 box of the P_{eps} promoter, and the +1 transcriptional start site of the eps operon are indicated by appropriately labelled grey boxes. Nucleotide positions relative to the transcriptional start site are indicated above the sequence at 20 bp intervals. Open boxes represent RemA binding sites (RemA BS1–6) as predicted from regions of DNase I protection by RemA–MBP presented in Fig. 4A. Black carets indicate regions of DNase I hyperdigestion caused by RemA–MBP presented in Fig. 4A. Dotted lines represent the regions of deleted bases corresponding to the Δ*remsite34* and Δ*remsite56* mutations as indicated. Bolded letters below the main line of sequence indicate the base substitutions identified by a forward genetic screen that abolished expression from a P_{eps}–*lacZ* reporter with the allele number in parentheses adjacent to the substitution. The delta symbol (Δ) represents the single base deletion found in the *eps32* allele.

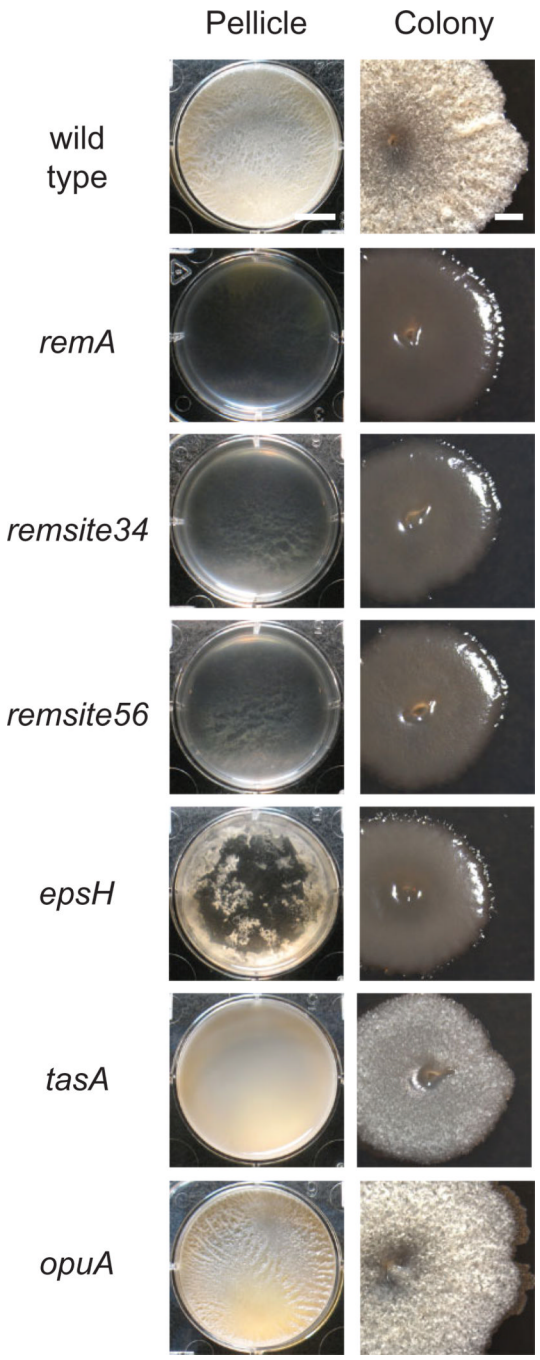

Fig. 6.

Deletion of RemA binding sites upstream of the P_{eps} promoter abolishes biofilm formation. 'Pellicle' column depicts microtitre wells (six-well plate) in which cells have been grown in MSgg medium for 3 days at 25°C. Scale bar is 1 cm. 'Colony' column depicts 10× images of individual colonies grown on MSgg medium for 3 days at 25°C. Scale bar is 1 mm. The following strains were used to generate this figure: wild type (3610), *remA* (DS2679), Δ*remsite34* (DS8402), Δ*remsite56* (DS8403), *epsH* (DS76), *tasA* (DS3323) and *opuA* (DK220).

Mol Microbiol. Author manuscript; available in PMC 2014 June 01.

Table 1

Genes activated by RemA.[a]

Gene	Fold	Annotation	Gene	Fold	Annotation
		(Biofilm genes)[b]			**(Miscellaneous cont.)**
epsA	136.5	EPS synthesis, length regulator?	*cgeA*	10.5	Spore coat protein
epsB	87.3	EPS synthesis, tyrosine kinase?	*cgeB*	4.3	Maturation of the spore coat
epsC	123.3	EPS synthesis, epimerase	*cotG*	9.8	Spore coat protein
epsD	120.1	EPS synthesis, glycosyltransferase	*cotJC*	4.2	Spore coat protein
epsE	136.3	EPS synthesis and flagellar clutch	*glgA*	3.6	Glycogen synthase
epsF	136.4	EPS synthesis, glycosyltransferase	*glgB*	3.5	1,4-a-glucan branching enzyme
epsG	142.3	EPS synthesis, unknown	*glgP*	3.6	Glycogen phosphorylase
epsN	4.8	EPS synthesis, aminotransferase	*sacT*	3.6	Transcriptional antiterminator
epsO	6.9	EPS synthesis, pyruvyltransferase	*sigL*	3.9	Sigma factor L
tapA	116.3	TasA anchoring protein	*sodF*	4.6	Superoxide dismutase
sipW	145.7	TapA/TasA signal peptidase	*spoVR*	3.6	Involved in spore cortex synthesis
tasA	112.5	Extracellular amyloid fibre	*spoVID*	4.0	Assembly of spore coat
slrR	35.4	Regulator motility/autolysin genes	*sqhC*	3.3	Squalene-hopene synthase
bslA	4.2	Extracellular matrix protein	*ycdA*	7.5	Unknown
		(Osmoprotection)	*ycsF*	3.6	Similar to lactam utilization protein
opuAA	54.1	Glycine betaine ABC transporter	*ycsG*	3.4	Similar to amino acid transporter
opuAB	44.4	Glycine betaine ABC transporter	*yfjB*	7.2	Unknown
opuAC	43.7	Glycine betaine ABC transporter	*yfjC*	6.3	Unknown
opuBA	16.0	Choline ABC transporter	*yfjD*	6.5	Unknown
opuBB	15.4	Choline ABC transporter	*yfjE*	4.2	Unknown
opuBC	11.0	Choline ABC transporter	*ykoL*	7.5	Unknown
opuBD	12.8	Choline ABC transporter	*ykzB*	7.9	Unknown
opuCA	11.3	Glycine betaine/choline transporter	*yobB*	5.3	Unknown
opuCB	9.9	Glycine betaine/choline transporter	*yozY*	5.0	Unknown
opuCC	4.3	Glycine betaine/choline transporter	*yqfZ*	4.7	Unknown
opuCD	5.6	Glycine betaine/choline transporter	*yrbD*	9.9	Putative alanine transporter
		(Nitrogen metabolism)	*ysnE*	3.4	Similar to acetyltransferase

Gene	Fold	Annotation	Gene	Fold	Annotation
ansZ	12.0	Asparaginase	*yueB*	4.6	Surface receptor for phage SPP1
bpr	7.6	Bacillopeptidase F	*yueC*	4.4	Unknown
frlM	5.2	Amino sugar permease	*yuiA*	16.3	Unknown
frlN	5.1	Amino sugar permease	*yuiB*	10.9	Unknown
ispA	7.4	Intracellular protease	*yukB*	5.2	Unknown
nasB	9.7	Nitrate reductase (electron transfer)	*yukC*	4.6	Unknown
nasC	10.2	Nitrate reductase (catalytic subunit)	*yukD*	5.3	Putative bacteriocin
nasD	7.5	Assimilatory nitrate reductase	*yukE*	3.7	Unknown
nasE	6.3	Assimilatory nitrate reductase	*yvbF*	4.6	Unknown
nasA	14.0	Nitrate transporter	*yvcB*	3.7	Unknown
nrgA	5.6	Ammonium transporter	*ywhK*	4.0	Unknown
nrgB	6.6	Nitrogen regulated PII protein	*ywqH*	4.6	Unknown
pnbA	7.8	Para-nitrobenzyl esterase	*ywqI*	4.3	Unknown
pucA	7.8	Xanthine dehydrogenase	*ywqJ*	4.4	Putative toxin
pucB	11.6	Xanthine dehydrogenase	*ywqK*	4.1	Unknown
pucC	11.3	Xanthine dehydrogenase	*ywqL*	3.5	Endonuclease V
pucD	7.5	Xanthine dehydrogenase	*ywrD*	8.6	Unknown
pucE	8.3	Xanthine dehydrogenase	*ywrK*	5.4	Similar to arsenic exporter
pucI	6.3	Allantoin permease	*ywzE*	9.5	Unknown
pucJ	4.3	Uric acid permease	*ywzF*	8.6	Unknown
pucK	5.2	Uric acid permease	*yxiB*	5.4	Unknown
pucL	7.2	Uricase	*yxiC*	6.6	Unknown
ureA	9.9	Urease	*yxiD*	4.6	Toxin
ureB	9.7	Urease	*yyzB*	5.1	Unknown
ureC	7.0	Urease			
vpr	3.1	Extracellular protease			

[a.] Microarray expression values of strain DS207 (*sinR epsH*) divided by microarray array expression values of strain DS9771 (*remA sinR epsH*).

[b.] Genes *epsH* through *epsM* in the *eps* operon failed to show a threefold change in expression presumably due to the integration of thetetracycline resistance gene inserted into the *epsH* gene (*epsH::tet*).

Genes assigned to functional categories in bold. (σ^D) indicates genes previously identified as being expressed under the control of σ^D (Serizawa *et al.*, 2004; Kearns and Losick, 2005).

Mol Microbiol. Author manuscript; available in PMC 2014 June 01.

Table 2

Genes inhibited by RemA.[a]

Gene	Fold	Annotation
		(σ^D-regulon)[b]
hag	4.9	Flagellin
hemAT	3.8	Methyl-accepting chemotaxis protein
lytD	3.5	Autolysin (glucosaminidase)
mcpA	3.9	Methyl-accepting chemotaxis protein
mcpC	3.1	Methyl accepting chemotaxis protein
pgdS	3.1	Gamma-DL-glutamyl hydrolase
tlpA	7.2	Methyl-accepting chemotaxis protein
ybdO	3.7	Unknown
yfmS	3.6	Methyl-accepting chemotaxis protein
ylqB	4.6	Unknown
yscB	3.6	Unknown
yxkC	14.4	Unknown
		(Miscellaneous)
braB	3.4	Amino acid transporter
comK	3.2	Transcriptional regulator of competence
sunA	3.3	Sublancin precursor
yjiC	4.6	Similar to macrolide glycosyltransferase
yomK	3.8	Unknown
yorD	4.2	Unknown
zinT	17.2	Unknown

[a] Microarray expression values of strain DS9771 (*remA sinR epsH*) divided by microarray array expression values of strain DS207 (*sinR epsH*).

[b] Genes previously identified as being expressed under the control of σ^D (Serizawa *et al.*, 2004; Kearns and Losick, 2005).

Table 3

Strains.

Strain	Genotype	Reference
3610	Wild type	
DK220	*opuA::tet*	
DS444	*sinI::spec amyE::*P_{eps}*–lacZ cat*	
DK445	*sinI::spec amyE::*$P_{eps}^{improved}$*–lacZ cat*	
DK549	*sinR::spec epsH::tet amyE::*P_{eps}^{14}*–lacZ cat*	
DK550	*sinR::spec epsH::tet amyE::*P_{eps}^{15}*–lacZ cat*	
DK551	*sinR::spec epsH::tet amyE::*P_{eps}^{32}*–lacZ cat*	
DK552	*sinR::spec epsH::tet amyE::*P_{eps}^{33}*–lacZ cat*	
DK553	*sinR::spec epsH::tet amyE::*P_{eps}^{40}*–lacZ cat*	
DK554	*sinR::spec epsH::tet amyE::*P_{eps}^{41}*–lacZ cat*	
DS76	*epsH::tet*	Kearns *et al.* (2005)
DS207	*sinR::spec epsH::tet*	Kearns *et al.* (2005)
DS1882	*epsH::tet amyE::*P_{eps}*–lacZ cat*	Kearns *et al.* (2005)
DS2609	*sinR::spec epsH::tet amyE::*P_{eps}*–lacZ cat*	Kearns *et al.* (2005)
DS2679	*remA::TnYLB kan*	Winkelman *et al.* (2009)
DS2911	*sinR::spec remA::TnYLB kan epsH::tet amyE::*P_{eps}*–lacZ cat*	Winkelman *et al.* (2009)
DS2913	*remA::TnYLB kan epsH::tet amyE::*P_{eps}*–lacZ cat*	Winkelman *et al.* (2009)
DS3323	*tasA::Tn10 spec*	
DS8402	Δ*remsite34*	
DS8403	Δ*remsite56*	
DS9466	*sinR::spec remA::TnYLB kan epsH::tet amyE::*$P_{eps}^{improved}$*–lacZ cat*	
DS9467	*sinR::spec epsH::tet amyE::*$P_{eps}^{improved}$*–lacZ cat*	
DS9468	*epsH::tet amyE::*$P_{eps}^{improved}$*–lacZ cat*	
DS9469	*remA::TnYLB kan epsH::tet amyE::*$P_{eps}^{improved}$*–lacZ cat*	
DS9771	*sinR::spec remA::TnYLB epsH::tet*	